The Journal of Cell Biology

Ca$^{2+}_{cyt}$ negatively regulates the initiation of oocyte maturation

Lu Sun and Khaled Machaca

Department of Physiology and Biophysics, University of Arkansas for Medical Sciences, Little Rock, AR 72205

Ca^{2+} is a ubiquitous intracellular messenger that is important for cell cycle progression. Genetic and biochemical evidence support a role for Ca^{2+} in mitosis. In contrast, there has been a long-standing debate as to whether Ca^{2+} signals are required for oocyte meiosis. Here, we show that cytoplasmic Ca^{2+} (Ca$^{2+}_{cyt}$) plays a dual role during *Xenopus* oocyte maturation. Ca^{2+} signals are dispensable for meiosis entry (germinal vesicle breakdown and chromosome condensation), but are required for the completion of meiosis I. Interestingly, in the absence of Ca$^{2+}_{cyt}$ signals oocytes enter meiosis more rapidly due to faster activation of the MAPK-maturation promoting factor (MPF) kinase cascade. This Ca^{2+}-dependent negative regulation of the cell cycle machinery (MAPK-MPF cascade) is due to Ca$^{2+}_{cyt}$ acting downstream of protein kinase A but upstream of Mos (a MAPK kinase kinase). Therefore, high Ca$^{2+}_{cyt}$ delays meiosis entry by negatively regulating the initiation of the MAPK-MPF cascade. These results show that Ca^{2+} modulates both the cell cycle machinery and nuclear maturation during meiosis.

Introduction

Mammalian and amphibian oocytes arrest at the G2/M border of the cell cycle after oogenesis (Yamashita et al., 2000). Before these oocytes become fertilization competent, they undergo a so-called "oocyte maturation" period during which they acquire the ability to activate in response to sperm entry, and to support the early stages of embryonic development (Yamashita et al., 2000). During maturation, oocytes progress through meiosis and arrest at metaphase of meiosis II until fertilization.

    Xenopus oocyte maturation provides a valuable model to elucidate the signal transduction cascade mediating meiosis entry and progression. In *Xenopus*, oocyte maturation is triggered by the hormone progesterone, which binds to a cell surface receptor and not the classical nuclear receptor/transcription factor. Progesterone leads to inhibition of cAMP-dependent PKA and translation of the proto-oncogene c-Mos, which induces the MAPK cascade culminating in the activation of maturation promoting factor (MPF; for review see Nebreda and Ferby, 2000). MPF is the central kinase that regulates meiotic progression, and consists of a catalytic p34^{cdc2} serine/threonine kinase subunit (Cdk 1), and a regulatory cyclin B subunit (Coleman and Dunphy,

1994). MPF is also activated by the removal of inhibitory phosphorylations by the Cdc25C phosphatase, which is induced by the polo-like kinase cascade (Nebreda and Ferby, 2000).

    A variety of genetic and biochemical evidence support a role for Ca^{2+}, and its downstream effectors CaM and Ca^{2+}-CaM–dependent protein kinase II, in mitosis initiation and progression (Means, 1994; Whitaker, 1995). Ca^{2+} signals are required for nuclear envelope breakdown (NEBD), and chromosome condensation during mitosis (Steinhardt and Alderton, 1988; Twigg et al., 1988; Kao et al., 1990; Tombes et al., 1992; Ciapa et al., 1994). Furthermore, the cytoplasmic Ca^{2+} (Ca$^{2+}_{cyt}$) rise observed at fertilization is the universal signal for egg activation in all species investigated (Stricker, 2000). Ca^{2+} signals at fertilization release the metaphase II arrest by activating proteolytic degradation of cytostatic factor, thus inducing completion of meiosis II and entry into the mitotic cell cycle (Tunquist and Maller, 2003). In addition, Ca^{2+} release at fertilization induces both the fast and slow blocks to polyspermy in *Xenopus* eggs (Machaca et al., 2001). In contrast to the well-defined roles for Ca^{2+} signals in mitosis and after

Address correspondence to Khaled Machaca, Dept. of Physiology and Biophysics, University of Arkansas for Medical Sciences, 4301 West Markham St., Slot 505, Little Rock, AR 72205. Tel.: (501) 603-1596. Fax: (501) 686-8167. email: kamachaca@uams.edu

Key words: calcium; meiosis; cell cycle; meiotic maturation; *Xenopus*

Figure 1.   **Role of extracellular and store Ca^{2+} load in GVBD.** (A) Oocytes were incubated in L-15 containing the indicated Ca^{2+} concentrations, stimulated with progesterone, and GVBD scored every half hour. (B) Cells were incubated in media with different calcium concentrations: low Ca^{2+} (L-Ca) 50 μM Ca^{2+}; normal Ca^{2+} (N-Ca) 0.6 mM Ca^{2+}; and high Ca^{2+} (H-Ca) 5 mM Ca^{2+}, and treated with either 2 μM thapsigargin for 3 h (Thap) or 10 μM ionomycin for 5 min (Ion) before progesterone addition. Control (Con) refers to cells incubated N-Ca and stimulated with progesterone. For the treatments described no GVBD was observed in the absence of progesterone, indicating that the different manipulation are not sufficient to induce maturation. (C) The rate of oocyte maturation, quantified as the time at which 50% of the oocytes have undergone GVBD (GVBD$_{50}$). The GVBD$_{50}$ for each indicated treatment were normalized to GVBD$_{50}$ in the N-Ca control. (D) Maximal percentage of cells that undergo GVBD for the different treatments. (C and D) Asterisks indicate significantly different means (P ≤ 0.0146, n = 6). (E and F) Prolonged Ca^{2+} store depletion does not inhibit GVBD. Oocytes were incubated with or without 2 μM thapsigargin for the times indicated (from 3 to 48 h) before progesterone addition. The rate of maturation (GVBD$_{50}$) and maximal GVBD are shown. For all experiments GVBD was directly confirmed by fixing and bisecting oocytes. Error bars are SEM.
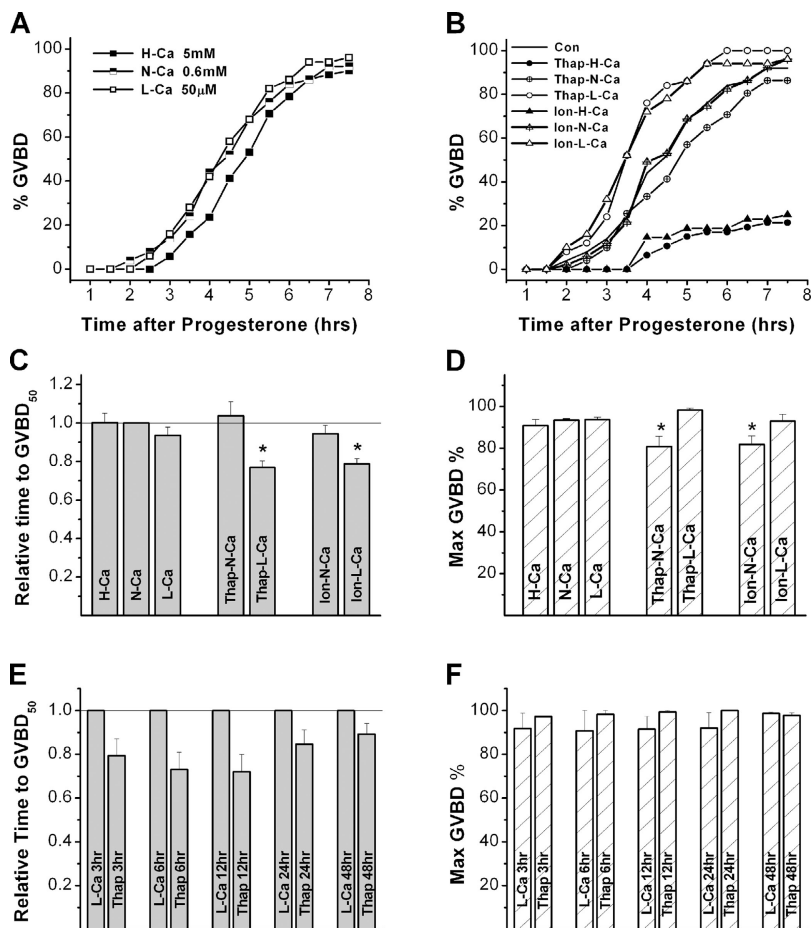
fertilization, the role of Ca^{2+} signals during oocyte maturation remains contentious.

There has been a long-standing debate in the literature as to whether Ca^{2+} signals are required for *Xenopus* oocyte maturation/meiosis (Duesbery and Masui, 1996). Early reports argued that a Ca$^{2+}_{cyt}$ rise is sufficient to induce oocyte maturation (Wasserman and Masui, 1975; Moreau et al., 1976; Schorderet-Slatkine et al., 1976). Furthermore, oocytes injected with high concentrations of Ca^{2+} buffers were unable to mature (Moreau et al., 1976; Duesbery and Masui, 1996). However, injection of IP$_3$, which induces Ca^{2+} release, did not stimulate meiotic maturation (Picard et al., 1985). Additional support for a Ca^{2+} role in oocyte maturation comes from reports that measured a Ca$^{2+}_{cyt}$ rise after progesterone addition using ^{45}Ca^{2+} as a tracer, Ca^{2+} imaging, or Ca^{2+}-sensitive electrodes (O'Connor et al., 1977; Moreau et al., 1980; Wasserman et al., 1980). In contrast, others could not detect Ca$^{2+}_{cyt}$ changes downstream of progesterone addition using similar techniques (Robinson, 1985; Cork et al., 1987). A role for CaM in *Xenopus* oocyte maturation has also been postulated (Wasserman and Smith, 1981) and challenged (Cicirelli and Smith, 1987). These conflicting reports argue that the relationship between Ca^{2+} and oocyte maturation is complex.

We decided to revisit the role of Ca^{2+} during oocyte maturation/meiosis by framing the problem in terms of the spatially distinct sources of Ca^{2+} signals. Ca$^{2+}_{cyt}$ signals can be generated either due to Ca^{2+} release from intracellular Ca^{2+} stores (ER) or Ca^{2+} influx from the extracellular space. In fact, these two Ca^{2+} sources are mechanistically linked through the store-operated Ca^{2+} entry (SOCE) pathway, which is activated in response to intracellular Ca^{2+} stores depletion. Therefore, Ca$^{2+}_{cyt}$ is regulated by the balance between Ca^{2+} release and Ca^{2+} influx. By manipulating Ca^{2+} store load and the extent of Ca^{2+} influx through SOCE, we show here that Ca^{2+} signals are not required for meiosis entry. On the contrary, high Ca$^{2+}_{cyt}$ delays meiosis entry. However, in the absence of Ca$^{2+}_{cyt}$ signals oocytes arrest in meiosis I, form abnormal spindles, and do not extrude a polar body. Surprisingly, MAPK and MPF kinetics in oocytes deprived of Ca^{2+} signals are normal. We further mapped the site of action of Ca$^{2+}_{cyt}$ on meiosis entry and show that Ca$^{2+}_{cyt}$ negatively regulates the cell cycle machinery by acting downstream of PKA and upstream of Mos. These data argue that Ca^{2+} signals regulate the timing of meiosis entry, and that they are required for the completion of meiosis I. The dual role of Ca$^{2+}_{cyt}$ revealed by these studies help explain some of the controversy surrounding the role of Ca^{2+} in oocyte maturation, and provides a framework to explore the role of Ca^{2+}-dependent signaling cascades in meiosis.

Results

Depleting intracellular Ca^{2+} stores accelerates entry into meiosis

Maturing oocytes in media with different Ca^{2+} concentrations ([Ca^{2+}]) does not affect the time course or extent of

germinal vesicle (nucleus) breakdown (GVBD; Fig. 1, A and C), which is indicative of meiosis entry. The rate of maturation in the population was quantified as the time required for 50% of the oocytes to undergo GVBD (GVBD$_{50}$). Because the rate and extent of GVBD were unaffected in low Ca²⁺ (L-Ca) medium, this shows that Ca²⁺ influx is not required for entry into meiosis (Fig. 1, C and D).

To test whether intracellular Ca²⁺ levels affect oocyte maturation, we emptied Ca²⁺ stores either by treating cells with thapsigargin, an inhibitor of the ER Ca²⁺ ATPase (SERCA), or with the Ca²⁺ ionophore ionomycin. Thapsigargin leads to Ca²⁺ store depletion because of a poorly defined Ca²⁺ leak pathway from the ER (Camello et al., 2002). Emptying Ca²⁺ stores activates Ca²⁺ influx through SOCE (Parekh and Penner, 1997). Because the extent of Ca²⁺ influx through SOCE depends on [Ca²⁺] in the medium, oocytes incubated in high Ca²⁺ (H-Ca) medium will have more Ca²⁺ influx than those in normal Ca²⁺ (N-Ca) medium, and no Ca²⁺ influx in expected in L-Ca medium (see Fig. 4).

Emptying Ca²⁺ stores with either thapsigargin or ionomycin in N-Ca does not affect the time to GVBD$_{50}$ (Fig. 1, B and C, Thap-N-Ca and Ion-N-Ca), but decreases maximal levels of GVBD (Fig. 1 D, Thap-N-Ca and Ion-N-Ca). In H-Ca, emptying Ca²⁺ stores results in high percentage of cellular degeneration due to excessive Ca²⁺ influx, thus prohibiting analysis of the rate of meiosis entry because GVBD$_{50}$ is rarely reached under these conditions (Fig. 1 B, Thap-H-Ca and Ion-H-Ca). In contrast, emptying Ca²⁺ stores in L-Ca medium accelerates the rate of maturation (Fig. 1, B and C, Thap-L-Ca and Ion-L-Ca), without affecting maximal maturation levels (Fig. 1 D, Thap-L-Ca and Ion-L-Ca). In L-Ca medium with Ca²⁺ stores depleted, oocytes are unable to generate Ca²⁺ signals after progesterone addition because Ca²⁺ stores are depleted and Ca²⁺ influx is prevented in L-Ca medium (see Fig. 4); nonetheless they enter meiosis at an accelerated rate. These data show that Ca²⁺ signals are not required for GVBD and argue that Ca²⁺$_{cyt}$ negatively regulates meiosis entry.

Although Ca²⁺ signals after progesterone addition are dispensable for GVBD, it is conceivable that Ca²⁺$_{cyt}$ signals generated before progesterone addition are required for meiosis entry. To determine whether this is the case, we depleted Ca²⁺ stores with thapsigargin and waited for extended periods of time before inducing maturation with progesterone. We reasoned that if Ca²⁺ signals are required for GVBD, the longer we wait after depriving oocytes of Ca²⁺ signals the less effective progesterone will be in inducing maturation. Depleting stores for as long as 48 h does not affect the extent of oocyte maturation (Fig. 1 F), but still enhances oocyte maturation rate (Fig. 1 E). These results support the conclusion that Ca²⁺ signals are not required for entry into meiosis.

Lowering Ca²⁺$_{cyt}$ levels accelerates meiosis entry

The more rapid maturation observed in L-Ca medium when Ca²⁺ stores are depleted, argues that Ca²⁺$_{cyt}$ negatively regulates meiosis entry. It follows then that buffering Ca²⁺$_{cyt}$ at low levels should also accelerate meiosis entry. This is indeed the case as injection of 500 μM 1,2-bis(2-aminophenoxy)ethane-*N,N,N',N'*-tetraacetic acid (BAPTA) alone or
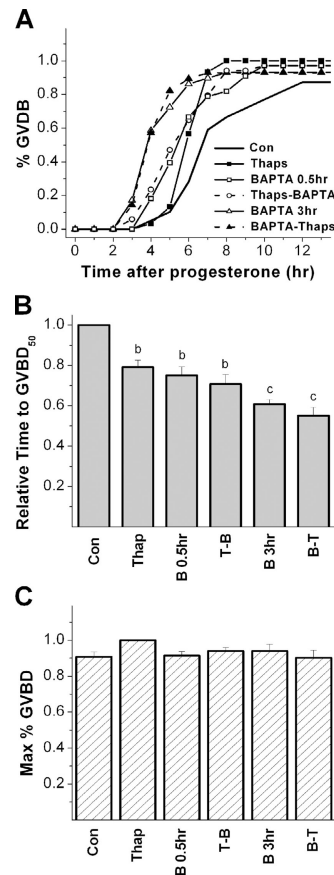

Figure 2.   **Buffering Ca²⁺$_{cyt}$ with BAPTA accelerates meiosis entry.** (A) GVBD time course of BAPTA-injected cells. Oocytes were incubated in L-Ca medium and treated in one of the following ways: injected with 500 μM BAPTA (BAPTA); incubated in 2 μM thapsigargin for 3 h (Thaps); or treated with both BAPTA and thapsigargin (Thaps-BAPTA) in the order and for the times indicated. The control group (Con) refers to 5 μg/ml of progesterone alone. (B and C) The rate of maturation (B, GVBD$_{50}$), and maximal GVBD (C) are shown for the different treatments. Letter designations refer to significantly different means (P < 0.018, $n = 5$).

in combination with thapsigargin in varying orders, results in a more rapid maturation (Fig. 2, A and B). BAPTA and thapsigargin treatments accelerate maturation to a similar extent with no significant additive effect. However, the longer the interval between BAPTA injection and progesterone addition the more rapid the maturation rate (Fig. 2 B). In all treatments the extent of maturation was comparable (Fig. 2 C). Similar results were obtained when BAPTA was injected at 1 mM (unpublished data). These data argue that at resting Ca²⁺$_{cyt}$ levels some Ca²⁺-dependent pathways are active and negatively regulate meiosis entry.

As reported by others, injecting high BAPTA concentrations (2.5–5 mM) blocks GVBD, arguing that Ca²⁺ is required for GVBD (Moreau et al., 1976; Duesbery and Masui, 1996). However, at such high BAPTA concentrations we observe significant levels of oocyte degeneration, bringing into question the specificity of this treatment. As shown below, injecting BAPTA at 500 μM effectively buffers Ca²⁺$_{cyt}$ transients (Fig. 4). In addition, depleting Ca²⁺ stores in the absence of extracellular Ca²⁺, thus depriving oocytes of Ca²⁺ signals, does not block GVBD. Furthermore, treating oocytes

Figure 3. **Effects of high Ca^{2+}$_{cyt}$ on meiosis entry.**
(A and B) GVBD time course of oocytes incubated in media containing increasing Ca^{2+} concentrations: 50 μM, 0.6 mM, 1.5 mM, 3 mM, and 5 mM for L-Ca, N-Ca, H1.5-Ca, H3-Ca, and H5-Ca, respectively, with (B) or without (A) thapsigargin (T) treatment (2 μM, 3 h). Oocytes with high Ca^{2+} (3 and 5 mM) had a diffuse white spot on the animal pole, but when fixed and cut the nucleus was present although flattened and close to the membrane. In addition, oocyte degeneration was observed in these treatments, which partly contributes to lower GVBD levels. No degeneration was seen in 1.5 mM Ca^{2+} (H1.5-Ca). (C and D) Relative GVBD$_{50}$ and maximal GVBD for the different treatments. For GVBD$_{50}$ (C) the letters above the bars indicate significantly different means (P < 0.05, n = 3). Oocytes in H3-Ca^{2+} and H5-Ca^{2+} are excluded from this analysis because they rarely reach GVBD$_{50}$. For maximal GVBD (D) the asterisk indicates significantly different means (P < 0.0155, n = 3).
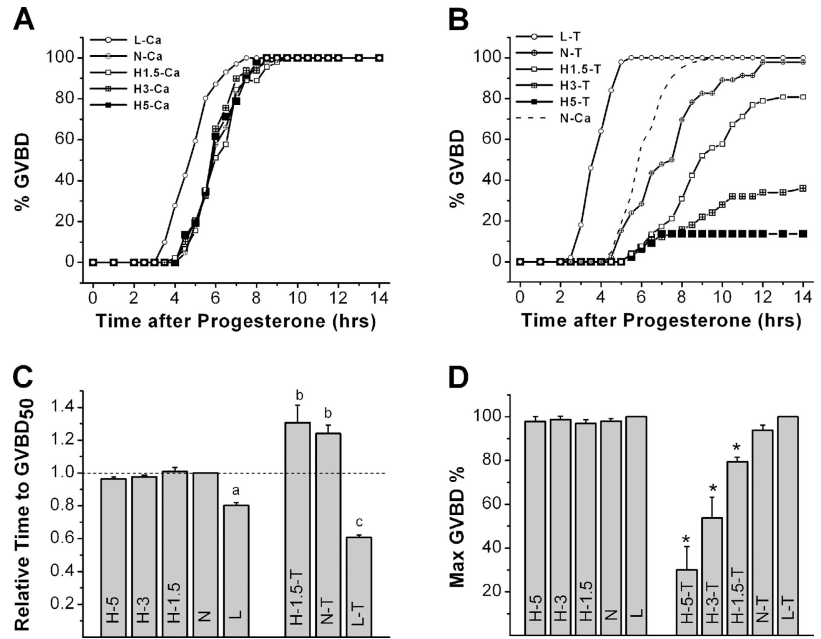
with the heavy metal chelator TPEN blocks oocyte maturation (unpublished data). Based on these findings, it is possible that high BAPTA concentrations block GVBD in a Ca^{2+}-independent manner, either due to a nonspecific effect of BAPTA, or chelation of other metal ions because BAPTA is a potent chelator of transition metals (Arslan et al., 1985).

High Ca^{2+}$_{cyt}$ delays meiosis entry

If Ca^{2+}$_{cyt}$ negatively regulates meiosis entry it is expected that raising Ca^{2+}$_{cyt}$ levels would lead to a slower rate of oocyte maturation. To test whether this is the case we induced different levels of Ca^{2+} influx through SOCE by depleting Ca^{2+} stores with thapsigargin and incubating oocytes with solutions containing 5 mM, 3 mM, 1.5 mM, 0.6 mM, and 50 μM Ca^{2+} (H-5, H-3, H-1.5, N-Ca, and L-Ca, respectively). Inducing maturation in solutions with different [Ca^{2+}] has no effect on the rate of oocyte maturation, except for L-Ca medium where maturation rate was more rapid (Fig. 3, A and C). Although this enhancement was more pronounced in this set of experiments, Fig. 1 shows a similar tendency toward a more rapid maturation in L-Ca medium. More importantly, after store depletion with thapsigargin, the higher the concentration of extracellular Ca^{2+} the slower the rate of maturation (Fig. 3, B and C). Furthermore, the extent of maturation was reduced in H-Ca containing solutions (H-5, H-3, and H1.5). At both 3 and 5 mM of extracellular Ca^{2+} (H-5 and H-3) some cellular degeneration was observed, but at 1.5 mM of extracellular Ca^{2+} the oocytes were healthy, but the rate of oocyte maturation was slower. These data show that the higher the level of Ca^{2+} influx the slower the rate of maturation, supporting the conclusion that high Ca^{2+}$_{cyt}$ levels negatively regulate meiosis entry.

Ca^{2+}-activated Cl$^-$ currents (I$_{Ca,Cl}$) as markers for Ca^{2+}$_{cyt}$ levels

To confirm that the different treatments are modulating Ca^{2+}$_{cyt}$ levels as predicted, we used endogenous Ca^{2+}-acti-

vated Cl$^-$ current (I$_{Cl,Ca}$), as an in situ marker of Ca^{2+}$_{cyt}$ levels (Fig. 4). We have shown previously that I$_{Cl,Ca}$ provides an accurate measure of both Ca^{2+} release and influx (Machaca and Hartzell, 1999). During Ca^{2+} release I$_{Cl,Ca}$ is activated as a sustained current (I$_{Cl1}$) at depolarized voltages (+40 mV; Fig. 4 A, left, trace t). I$_{Cl1}$ is sustained because during Ca^{2+} release Ca^{2+}$_{cyt}$ levels remain high for the duration of the voltage pulse. In contrast, during Ca^{2+} influx I$_{Cl,Ca}$ is activated as a transient current (I$_{CIT}$) only when the +40 mV pulse is preceded by a hyperpolarization step (−140 mV) to induce Ca^{2+} influx (Fig. 4 A, right, traces w–z). I$_{CIT}$ is transient because Ca^{2+} flows into the cell during the preceding −140 mV pulse, and then dissipates rapidly resulting in current inactivation (Machaca and Hartzell, 1999). We have shown using simultaneous electrical recording and Ca^{2+} imaging that I$_{Cl,Ca}$ faithfully reports the levels and kinetics of Ca^{2+} release and influx (Machaca and Hartzell, 1999). However, it is important to note that although I$_{Cl,Ca}$ provides an accurate measure of Ca^{2+} release and Ca^{2+} influx, it does not directly reflect Ca^{2+} levels deep in the cytosol as these channels localize to the plasma membrane.

To determine store Ca^{2+} load in the different treatments, we incubated oocytes in Ca^{2+}-free Ringer (F-Ca), and depleted Ca^{2+} stores with ionomycin. Because no Ca^{2+} influx is possible in Ca^{2+}-free solution, the level of I$_{Cl1}$ activated in response to ionomycin provides a measure of the extent of store Ca^{2+} load (Fig. 4, A and B). After the dissipation of the Ca^{2+} release transient indicated by the return of I$_{Cl1}$ to baseline (Fig. 4 B, squares), oocytes were sequentially exposed to L-Ca, N-Ca, H1.5-Ca, H3-Ca, and H5-Ca to determine the extent of Ca^{2+} influx (Fig. 4, B, D, and F). This protocol was applied to control untreated oocytes (Fig. 4 B) or to oocytes incubated in thapsigargin to fully deplete Ca^{2+} stores (Fig. 4 D), or injected with 500 μM BAPTA (Fig. 4 F). The levels of Ca^{2+} release as indicated by I$_{Cl1}$ and the levels of Ca^{2+} influx as indicated by I$_{CIT}$ were quantified in the different treatments (Fig. 4, C, E, and G). In control oocytes ion-
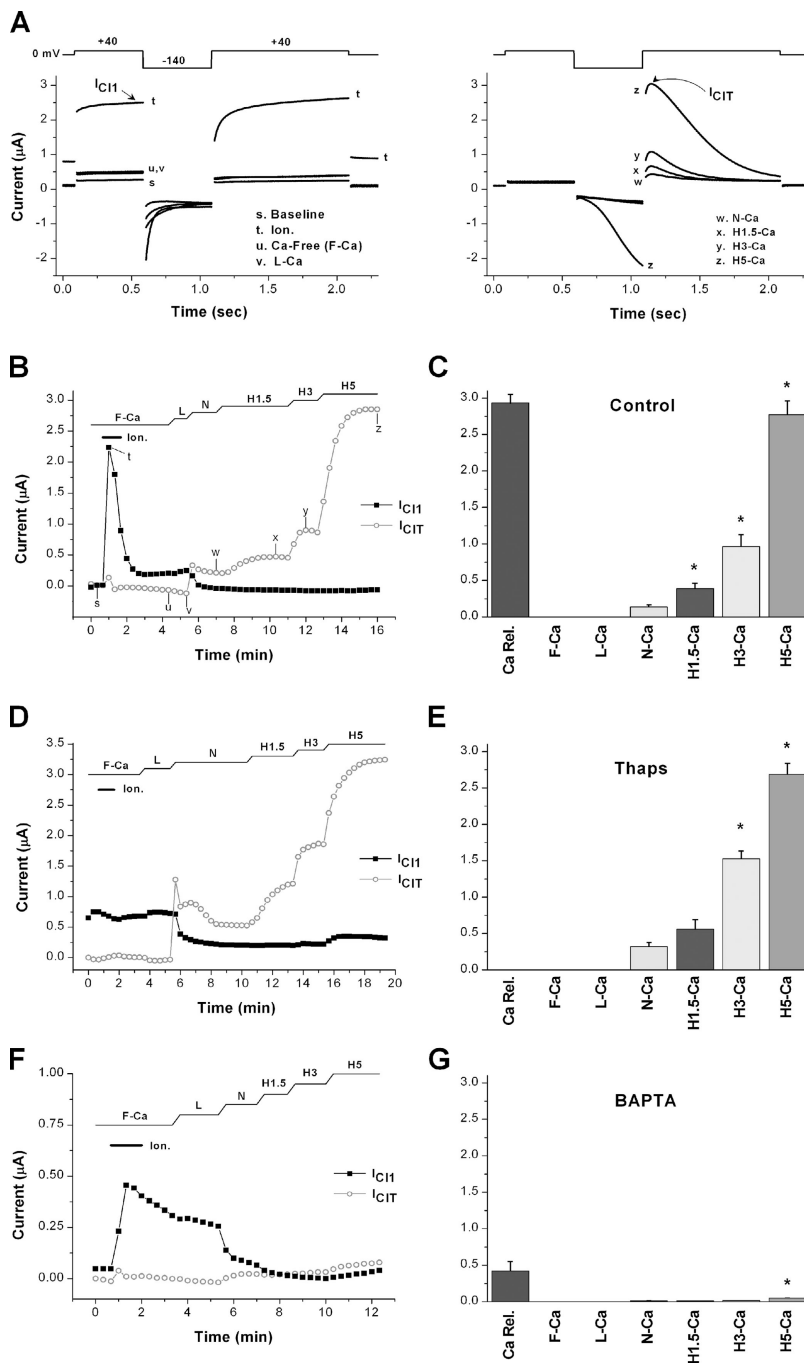
Figure 4.   **$I_{Ca,Cl}$ as marker for Ca^{2+}_{cyt} levels.** $I_{Ca,Cl}$ was recorded from control cells (untreated), cells treated with thapsigargin (2 μM, 3 h), or injected with 500 μM BAPTA to estimate store Ca^{2+} load and the levels of Ca^{2+} influx. $I_{Ca,Cl}$ provide endogenous reporters of Ca^{2+} release from stores (I_{Cl1}) and Ca^{2+} influx from the extracellular space (I_{CIT}) as described in the text. (A) Voltage protocol and representative current traces of the $I_{ca,Cl}$. I_{Cl1} is a sustained current recorded upon depolarization to +40 mV (trace t), whereas I_{CIT} is a transient current detected only when the +40 mV pulse is preceded by a hyperpolarization step to −140 mV (traces x–z). Note that at high 5 mM Ca^{2+} levels, Ca^{2+} influx at −140 mV activates an inward Cl^- current (trace z). The current traces shown are from the control oocyte in B. The time at which each trace was obtained is indicated in B. (B–G) Oocytes were incubated in Ca^{2+}-free Ringer (F-Ca) and treated with ionomycin to release store Ca^{2+}. The levels of I_{Cl1} induced in response to ionomycin provide a measure of store Ca^{2+} load. I_{Cl1} (squares) is plotted as the maximal current at the end of the +40 mV pulse as indicated by the arrow in A (left). After store depletion oocytes were sequentially exposed to solutions containing the indicated Ca^{2+} concentration: L (50 μM Ca^{2+}), N (0.6 mM Ca^{2+}), H1.5 (1.5 mM Ca^{2+}), H3 (3 mM Ca^{2+}), and H5 (5 mM Ca^{2+}). Store depletion activates Ca^{2+} influx through the SOCE pathway, which activates I_{CIT}. I_{CIT} (circles) is plotted as the maximal current during the second +40 mV pulse as indicated by the arrow in A (right). B, D, and F show the time course of I_{Cl1} and I_{CIT} in control, thapsigargin, and BAPTA-treated cells, respectively. The time of solution changes and ionomycin (Ion.) addition are indicated above each panel. C, E, and G show statistical analysis of I_{Cl1} and I_{CIT}. I_{Cl1} levels were significantly different in the three treatments (P ≤ 0.0041, n = 5–7). No I_{Cl1} was detected in the thapsigargin treatment indicating complete Ca^{2+} store depletion. For I_{CIT} in each panel the asterisks indicate significantly different means: (C) Con, P ≤ 0.015, n = 5; (E) Thaps, P ≤ 0.00012, n = 7; (G) BAPTA, P = 0.00022, n = 6.

omycin activates a large I_{Cl1}, indicating that Ca^{2+} stores are fully loaded (Fig. 4 B, squares; Fig. 4 C, Ca Rel.). Ca^{2+} release leads to store depletion which activates SOCE. As expected, no I_{CIT} is detected in either Ca^{2+}-free solution (F-Ca) or in L-Ca medium (L-Ca) confirming our prediction that at 50 μM of extracellular Ca^{2+} no Ca^{2+} influx occurs (Fig. 4 B, circles; Fig. 4 C). Increasing levels of Ca^{2+} influx (indicated by I_{CIT}) are observed in media with increasing [Ca^{2+}] (Fig. 4 B, circles; Fig. 4 C; Fig. 4 A, right).

Oocytes treated with thapsigargin did not release Ca^{2+} in response to ionomycin as no I_{Cl1} was activated (Fig. 4 D, squares; Fig. 4 E, Ca Rel.), showing that Ca^{2+} stores were depleted. Because thapsigargin depletes Ca^{2+} stores, it activates Ca^{2+} influx through SOCE. As for control oocytes no

Ca^{2+} influx is observed in F-Ca or L-Ca solutions, and higher levels of Ca^{2+} influx, as indicated by I_{CIT}, are detected in solutions containing increasing Ca^{2+} (Fig. 4 D, circles; Fig. 4 E). Ca^{2+} influx levels in thapsigargin-treated cells were similar to those in control cells (Fig. 4, C and E).

BAPTA injection dramatically reduces both Ca^{2+} release (I_{Cl1}) and Ca^{2+} influx (I_{CIT}) transients (Fig. 4, F and G). Small levels of Ca^{2+} release are observed in BAPTA-injected cells (Fig. 4 F, squares; Fig. 4 G, Ca Rel.), indicating that Ca^{2+} stores still contain Ca^{2+}, but that as Ca^{2+} is released it is chelated by BAPTA, thus drastically reducing the levels of free Ca^{2+} available to activate $I_{Ca,Cl}$. The same is true during the Ca^{2+} influx phase in different [Ca^{2+}] (Fig. 4, F and G). No Ca^{2+} influx can be detected in L-Ca solution, and small

Figure 5. **MPF and MAPK kinetics.** (A) GVBD time course for oocytes incubated in N-Ca, L-Ca, or treated with 2 μM of thapsigargin for 3 h or injected with 500 μM BAPTA. (B and C) Phospho-MAPK (P-MAPK; B) and MPF activity (C) in the different treatments. At each time point as indicated, lysates were assayed for P-MAPK levels using an anti–P-MAPK specific antibody, and for MPF levels measured as histone H1 kinase activity. MAPK and MPF assays were performed on the same lysate. For P-MAPK Western blots were also probed for α-tubulin (Tub) to provide a loading control. The time course is divided into two phases: (1) after progesterone addition and (2) after GVBD. The 50 and 37 molecular weight markers are shown on the left of each gel. These data are representative of three similar experiments.
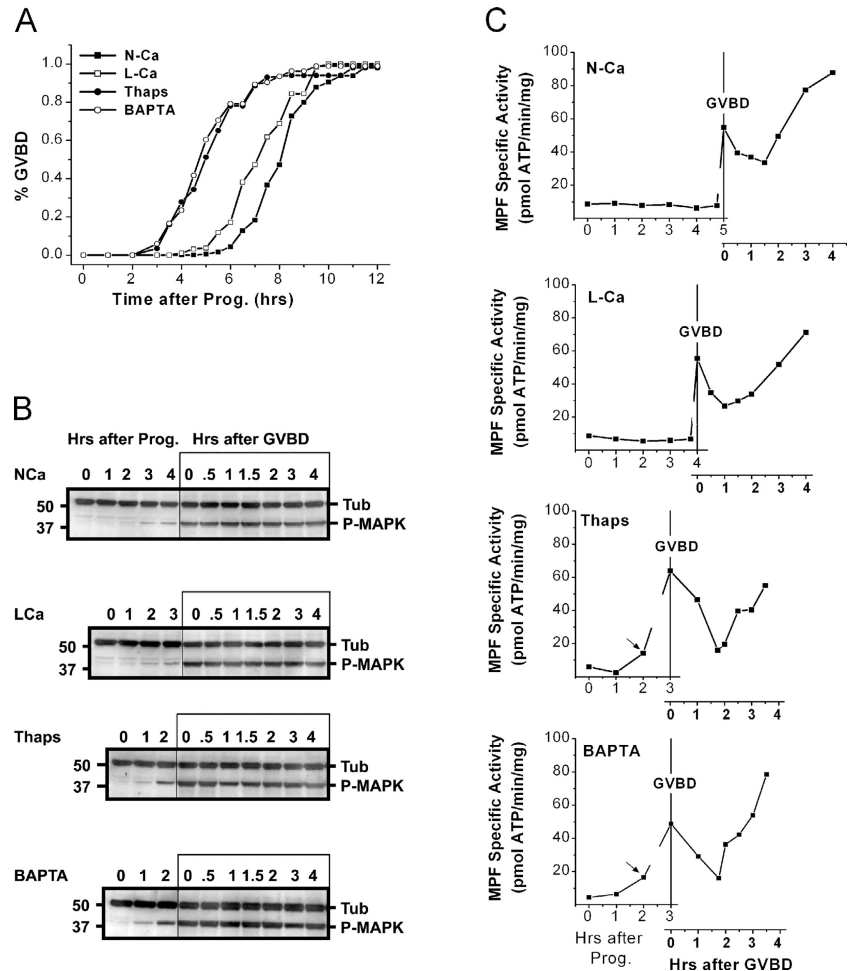
levels of I_{CIT} are observed in N-Ca through H3-Ca. Only H5-Ca produced evident, but small I_{CIT} consistently (Fig. 4 G). This indicates that the primary effect of BAPTA injection is to buffer Ca^{2+}_{cyt} at low levels. The fact that BAPTA injection enhances the rate of meiosis entry in a similar fashion to store depletion argues that this enhancement is due to a reduction of Ca^{2+}_{cyt} levels. It is noteworthy that Ca^{2+} store depletion has been shown to alter ER protein expression (Soboloff and Berger, 2002), however, based on the BAPTA data and the delayed maturation rate with high Ca^{2+}_{cyt}, it is unlikely that this is affecting meiosis entry.

Kinetics of MAPK and MPF activation

We assayed the rate and extent of oocyte maturation above based on the GVBD time course. GVBD marks entry into meiosis but does not provide any information about meiosis progression. Oocyte maturation is considered complete once oocytes reach metaphase of meiosis II. Although, the data presented so far show that Ca^{2+} signals are not required for entry into meiosis, they do not address whether meiosis/oocyte maturation can progress normally in the absence of Ca^{2+} signals. To determine whether interfering with Ca^{2+} signaling pathways affects meiosis progression, we tested the activation kinetics of the MAPK-MPF kinase cascade, which regulates meiosis transitions (Nebreda and Ferby, 2000). As described above (Figs. 1 and 2), treating cells with either

thapsigargin or injecting BAPTA accelerates meiosis entry (Fig. 5 A). In N-Ca medium, MAPK phosphorylation is first detected 2 h before GVBD, peaks at GVBD, and remains high for the remainder of maturation (Fig. 4 B, N-Ca). MAPK activates with similar kinetics in L-Ca, or after the thapsigargin (Thaps) or BAPTA treatments (Fig. 5 B). However, consistent with the GVBD time course, MAPK activated 1 h earlier in L-Ca medium and 2 h earlier after thapsigargin or BAPTA treatments (Fig. 5 B). These data show that in the absence of Ca^{2+} signals MAPK is induced earlier, but has normal kinetics after GVBD.

MPF activates in a characteristic fashion during oocyte maturation with a sharp peak at GVBD followed by a decline to an intermediate level that is indicative of the meiosis I to meiosis II transition, and rises again as oocytes progress through meiosis II (Fig. 4 C, N-Ca). MPF activity in oocytes matured in L-Ca medium follows the same kinetics except that peak MPF activity (GVBD) occurs ~1 h earlier than in N-Ca. This is consistent with the MAPK activation kinetics (Fig. 5 B) and the rate of GVBD (Fig. 5 A). MPF kinetics in the thapsigargin and BAPTA treatments are normal, except that, as for GVBD and MAPK, MPF activity peaks 2 h earlier than in the N-Ca treatment (Fig. 5 C, Thaps and BAPTA). Interestingly, an increase in MPF activity is detected as early as 1 h before GVBD (Fig. 5 C, Thaps and BAPTA, arrows). Such a premature activation of MPF is never observed in
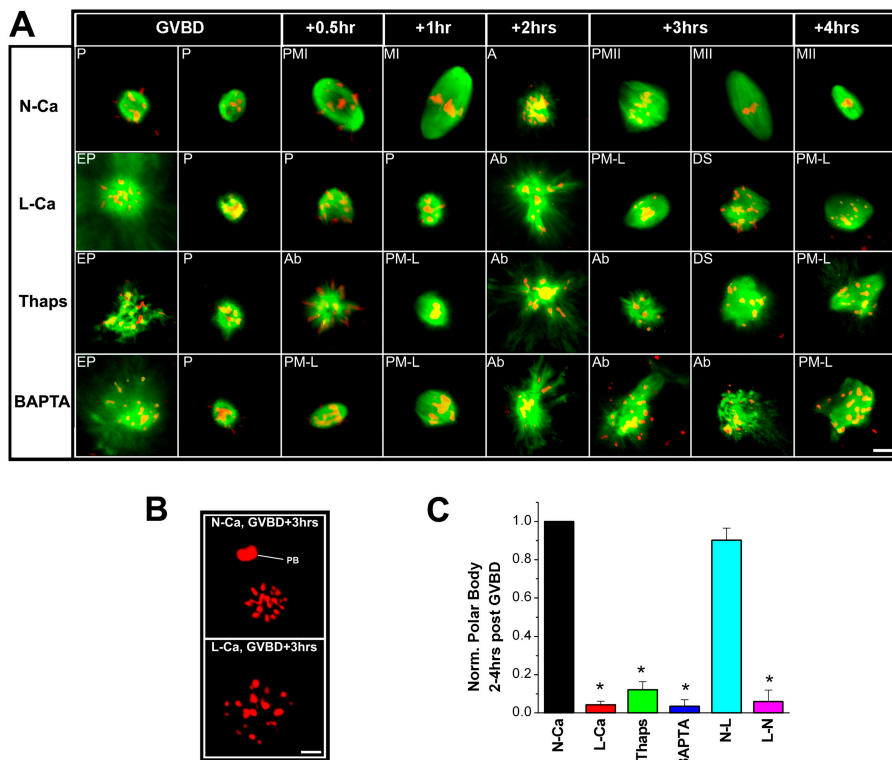
Figure 6. **Spindle structure.** Oocytes were stained for tubulin and DNA with Sytox orange to visualize spindle structure. (A) The treatment designation for N-Ca, L-Ca, Thaps, and BAPTA is as indicated in Fig. 5. P refers to cells in late prophase with clustering of the microtubules and chromosome condensation. PMI, prometaphase I; MI, metaphase I; A, Anaphase I; PMII, prometaphase II; MII, metaphase II; EP, early prophase with chromosome condensation but microtubules still spread over a large area; Ab, abnormal spindle structure; PM-L, prometaphase-like spindle with short or slightly disorganized structure; DS, double spindle with two overlapping spindles. (B and C) Polar body extrusion. (B) Representative images showing an oocyte with a polar body (PB) matured in N-Ca medium 3 h after GVBD (top); and an oocyte matured in L-Ca medium 3 h after GVBD, with no polar body (bottom). (C) Normalized polar body emission levels from 2–4 h after GVBD in the different treatments: N-Ca (0.6 mM); L-Ca (50 μM); thapsigargin (Thaps, 2 μM for 3 h); injected with 500 μM BAPTA (BAPTA); incubated in N-Ca until GVBD and then switched to L-Ca medium (N-L); or incubated in L-Ca until GVBD and then switched to N-Ca (L-N). Asterisks above the bar indicate significantly different means from N-Ca and N-L (P < 0.002; n = 3). Bars, 10 μm.

N-Ca or L-Ca. Therefore, MAPK and MPF activation kinetics (Fig. 5, B and C) correlate well with each other and with the rate of GVBD (Fig. 5 A), and show that reducing Ca^{2+}_{cyt} transients leads to premature activation of the MAPK-MPF kinase cascade. This premature activation explains the accelerated maturation rate in treatments that reduce Ca^{2+}_{cyt} transients. Therefore, Ca^{2+}_{cyt} modulates meiosis entry by negatively regulating the MAPK-MPF cascade.

Spindle formation and nuclear maturation

Kinase data in oocytes deprived of Ca^{2+} signals (Thaps and BAPTA) suggest that in the absence of Ca^{2+}_{cyt} signals meiosis proceeds normally after GVBD. To determine whether this is the case we imaged meiotic spindle structure and chromosome dynamics in oocytes matured in N-Ca, L-Ca, and oocytes treated with thapsigargin or BAPTA (Fig. 6). This allowed us to assess the progression of nuclear maturation, and directly compare it to MPF, MAPK, and GVBD kinetics because all three experiments were performed on the same batch of oocytes.

Control oocytes matured in N-Ca medium progress normally through meiosis (Fig. 6 A, Table I, N-Ca). At GVBD oocytes were at the late prophase I stage (Fig. 6 A, N-Ca, P), which refers to oocytes that have undergone GVBD, have condensed chromosomes, and organized microtubules around the chromosomes, but have not yet formed a bipolar spindle (Fig. 6 A, N-Ca, P). At 0.5 h after GVBD prometaphase I structures (30%; Table I) are observed with a typical bipolar spindle and associated chromosomes (Fig. 6 A, N-Ca, PM I).

This is followed by metaphase I with chromosome lined up at the metaphase plate (Fig. 6 A, N-Ca, M I) at ∼1 h after GVBD (Table I). Between 2–4 h after GVBD oocytes progress from M I to metaphase II (Table I) at which stage they arrest. Examples of anaphase I (A), prometaphase II (PM II), and metaphase II spindles are shown in Fig. 6 A (N-Ca).

Surprisingly, oocytes matured in L-Ca medium alone or treated with thapsigargin or BAPTA formed abnormal spindles. The progression through meiosis was not significantly different between the three treatments which will be discuss as a group. At GVBD a large percentage of these oocytes (≥57%; Table I) had condensed chromosomes, but the microtubule were still dispersed over a large area. We refer to this stage as early prophase (EP; Fig. 6 A), because eventually these oocytes do progress to the late prophase stage (P) as described for the control group (N-Ca) above (Table I). However, oocytes matured in L-Ca medium or treated with BAPTA or thapsigargin rarely progress to prometaphase I and never reach metaphase I (Fig. 6 A; Table I). Instead, they form abnormal structures at different rates depending on the treatment as detailed in Table I. Based on the severity of defects we divided abnormal spindles into three groups: (1) We refer to small and/or slightly disorganized spindles as prometaphase like (PM-L; Fig. 6 A). These spindles are the least disorganized and are observed throughout the time period studied (Table I). (2) The second group represents completely disrupted spindles (Ab) with no clear structure and with the microtubules highly condensed and/or spread over a large area. In most but not all instances condensed chromosomes were still

Table I. **Meiosis progression after interfering with Ca^{2+} signaling**

Treatment	Time[a]	Stage of meiosis						Abnormal spindles		
		Early prophase (EP)	Late prophase (P)	Prometaphase I (PM I)	Metaphase I (M I)	Anaphase I–Prometaphase II (A I–PM II)	Metaphase II (M II)	Prometaphase-like (PM-L)	Disrupted (Ab)	Double spindle (DS)
	h									
N-Ca	0		1 (5/5)							
	+0.5		0.7 (7/10)	0.3 (3/10)						
	+1			0.55 (5/9)	0.44 (4/9)					
	+2					1 (13/13)				
	+3					0.59 (10/17)	0.41 (7/17)			
	+4					0.5 (5/10)	0.5 (5/10)			
L-Ca	0	0.8 (4/5)	0.2 (1/5)							
	+0.5		1 (10/10)							
	+1		0.86 (12/14)						0.14 (2/14)	
	+2		0.13 (2/15)						0.87 (13/15)	
	+3		0.24 (4/17)	0.18 (3/17)					0.29 (5/17)	0.29 (5/17)
	+4							0.33 (2/6)	0.5 (3/6)	0.17 (1/6)
Thaps	0	0.57 (4/7)	0.43 (3/7)							
	+0.5		0.64 (7/11)						0.36 (4/11)	
	+1							0.43 (3/7)	0.67 (6/9)	
	+2								1 (15/15)	
	+3							0.28 (5/18)	0.67 (12/18)	0.05 (1/18)
	+4							0.44 (7/16)	0.56 (9/16)	
BAPTA	0	0.5 (5/10)	0.5 (5/10)							
	+0.5	0.09 (1/11)	0.64 (7/11)					0.27 (3/11)		
	+1		0.13 (2/15)					0.47 (7/15)	0.4 (6/15)	
	+2							0.4 (4/10)	0.6 (6/10)	
	+3								1 (6/6)	
	+4							0.37 (3/8)	0.63 (5/8)	

The number of oocytes analyzed is shown in parentheses.
[a]At each time point at (time 0) and after GVBD, the fraction of oocytes at the indicated stage of meiosis is shown. Stages of meiosis were determined based on spindle structure (Fig. 6).
EP: GVBD occurred; chromosomes condensed; MT disorganized over a large area. P: Chromosomes condensed; MT organized in small area (early spindle). A I–PM II: Meiotic stages between anaphase I and prometaphase II. Anaphase and telophase I typically exhibit disorganized MT during chromosome separation. Prophase and prometaphase II are defined as prometaphase-like structures that were preceded by M I at earlier time points. PM-L: Short or slightly disorganized spindle with condensed chromosomes. Ab: Spindle disrupted with MT highly condensed; some MT depolimerization; spiky MT. DS: Two overlapping spindles.

associated with the disrupted spindle (Fig. 6 A, Ab). (3) The last and most interesting group we refer to as the double spindle (DS) group (see Fig. 6 A). These double spindles were most common in the L-Ca group (Table I), but were also observed in the thapsigargin treatment (Fig. 6 A, Thaps, DS).

It is interesting that the highest percentage of disrupted spindles (Ab) in the experimental groups (L-Ca, Thaps, and BAPTA) is observed at 2–3 h after GVBD which corresponds to the meiosis I to meiosis II transition in control oocytes. At later time points, spindle structures are improved (PM-L), as if the cells are attempting to go through meiosis II. This is supported by the appearance of DS structures at 3–4 h after GVBD arguing that although these oocytes do not progress normally through meiosis I, they attempt to form a meiosis II spindle, that in some cases lead to the observed double-spindle structures. This might be expected with normal MAPK and MPF kinetics past GVBD in all the treatments (Fig. 5), which will drive these cells into meiosis II despite the abnormal progression through meiosis I. The fact that MPF and MAPK kinetics are normal past GVBD in the L-Ca, thapsigargin, and BAPTA treatments (Fig. 5), but that meiotic spindles are disorganized show that interfering with Ca^{2+} signaling during meiosis uncouples the MAPK-MPF cascade from spindle structure regulation. Furthermore, these results show that although Ca^{2+} signals are not required for meiosis entry (GVBD and chromosome condensation), they are necessary for progression through meiosis I and for bipolar spindle formation.

Polar body emission

Spindle structure data show that interfering with Ca^{2+} signaling leads to abnormal spindles, arguing that oocytes do not complete meiosis I. To directly confirm this, we assessed polar body emission from 1–4 h after GVBD in the different treatments (Fig. 6, B and C). In N-Ca medium, polar bodies were observed in the majority of the cells, but as expected from the spindle structure experiments, oocytes matured in L-Ca medium or treated with thapsigargin or BAPTA rarely extrude a polar body (Fig. 6 C). This shows that interfering with Ca^{2+} signaling inhibits the completion of meiosis I.

The fact that oocytes matured in L-Ca medium had abnormal spindle structure and could not finish meiosis I argues that either Ca^{2+} influx from the extracellular space is required during the early stages of oocytes maturation for normal meiosis progression, or that oocytes are unable to form a polar body at low extracellular Ca^{2+}. To differentiate
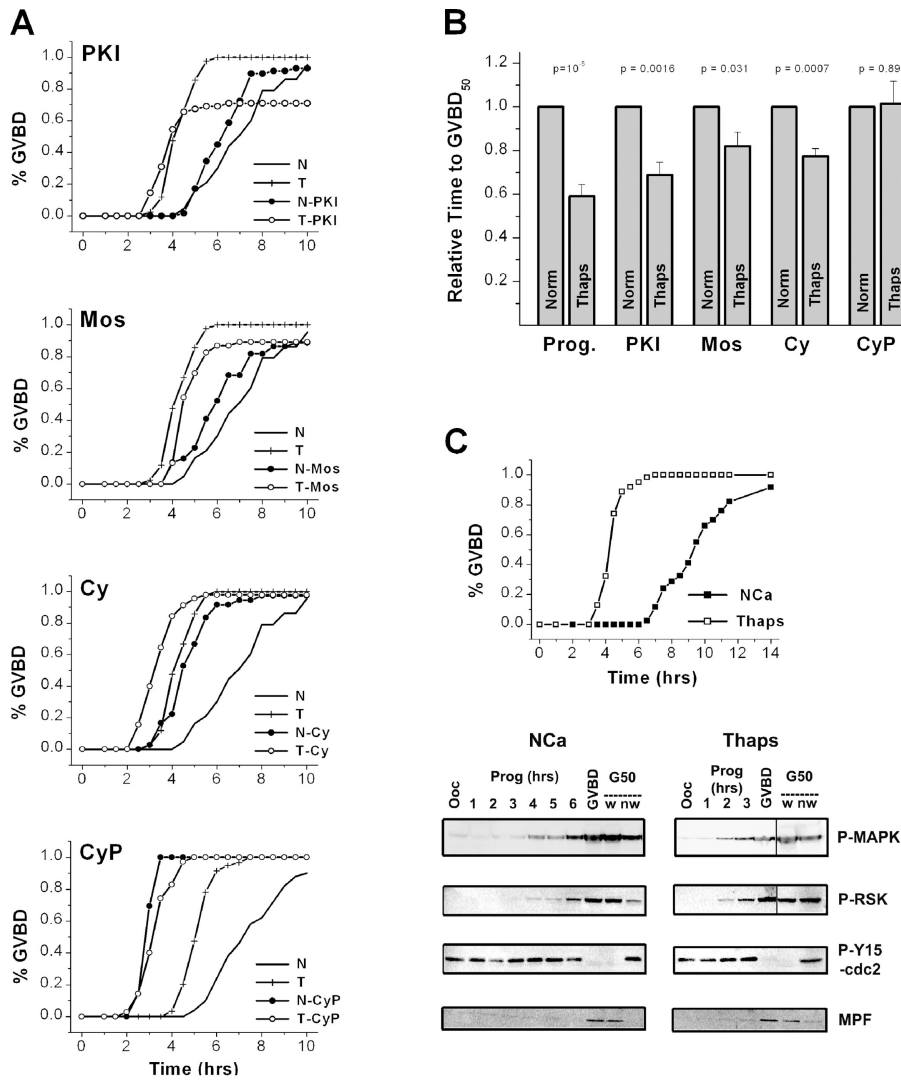
Figure 7. **Mapping the site of action of Ca²⁺$_{cyt}$ on meiosis entry.** (A) GVBD time course for oocytes incubated in N-Ca solution (N), or L-Ca, and treated with thapsigargin (T). Oocyte maturation was induced with progesterone (N and T), PKI (PKI), Mos RNA 10 ng (Mos), cyclin B1 RNA 10 ng (Cy), or Δ87cyclin B1 protein ∼200 pg (CyP). (B) Relative time to GVBD$_{50}$ normalized to GVBD$_{50}$ in the N-Ca for each activator. P values are shown above the graph, n = 4–7. (C) Biochemical analysis of the cell cycle machinery. Maturation was induced as described in A and lysates were collected from immature oocytes (ooc), at hourly intervals after progesterone addition as indicated, at first GVBD (GVBD) and at GVBD$_{50}$ (G50). For the GVBD$_{50}$ time point we collected lysates form oocytes that have undergone GVBD (white spot, w) and those that have not (no white spot, nw). (D) Working model for the role of Ca²⁺$_{cyt}$ in oocyte maturation/meiosis (see text for details). Dashed arrows indicated yet unknown steps in the cascade. The change in arrow shape and the bold font indicate transitions between the different stages of meiosis. M I, meiosis I; PB, polar body emission; M II, meiosis II.

between these possibilities we assessed polar body emission in oocytes incubated in N-Ca solution until GVBD and then switched to L-Ca solution (N-L); or in oocytes incubated in L-Ca solution until GVBD and then switched to N-Ca medium (L-N). Oocytes in the N-L group, but not the L-N group, emitted polar bodies to the same extent as the N-Ca control group (Fig. 6, B and C), arguing that Ca²⁺ influx in the early stages of oocyte maturation is required for meiosis I progression.

Ca²⁺$_{cyt}$ acts between PKA and Mos to negatively regulate entry into meiosis

To better define the mechanism by which Ca²⁺$_{cyt}$ negatively regulates meiosis entry, we mapped the site of action of Ca²⁺$_{cyt}$ on the cell cycle machinery using an epistatic ap-

proach. For these experiments thapsigargin-treated oocytes represented the experimental group deprived of Ca²⁺ signals. Control oocytes were activated in N-Ca solution. Our approach was to activate the cell cycle machinery at different points along the MAPK-MPF signal transduction cascade, and determine whether the enhancing effect of Ca²⁺ deprivation on the rate of maturation is still observed. Oocytes were activated with progesterone, or by injection of an inhibitor of PKA inhibitor (PKI), Mos RNA (Mos), cyclin B1 RNA (Cy) and Δ87cyclin B1 protein (CyP; Fig. 7 A). Thapsigargin treatment enhanced the rate of oocyte maturation to a similar extent in oocytes activated with progesterone or PKI (Fig. 7 A, PKI). Thapsigargin-treated oocytes activate faster than controls after Mos RNA injection, but the effect on Ca²⁺ deprivation on the rate of maturation is smaller than

in the case of progesterone (Fig. 7 A, Mos). Because the kinetics of the kinase cascade downstream of Mos are similar in control and thapsigargin-treated oocytes (Fig. 7 C; Fig. 5), we wondered whether the faster maturation rate in thapsigargin-treated Mos-injected oocytes is due to an effect of Ca^{2+} deprivation on RNA translation. To determine whether this is the case we induced meiosis by directly activating MPF through the expression of cyclin B1 to activate the free cdc2 pool in the oocyte. Similar to Mos RNA injection, thapsigargin-treated oocytes activated faster than controls after cyclin B1 RNA injection (Fig. 7 A, Cy). In contrast, injecting oocytes with cyclin B1 protein induces GVBD with a similar time course in both thapsigargin-treated and control oocytes (Fig. 7 A, CyP). The rate of oocyte maturation with the different activators is summarized in Fig. 7 B. Because the rate of maturation varies between activators we normalized maturation rate for each activator to the rate of activation in N-Ca (Fig. 7 B) to allow a better visualization of the relative effect of Ca^{2+} deprivation on maturation. For example, although cyclin B activates maturation faster than Mos (Fig. 7 A), the relative enhancement in the rate of maturation (~20% faster) is similar between the two activators in the absence of Ca^{2+} signals (Fig. 7 B). This argues that the more rapid maturation in oocytes deprived of Ca^{2+} signals after both Mos and cyclin RNA injections is due to an effect of Ca^{2+}_{cyt} on translation of the injected RNAs. This conclusion is supported by the fact that control and thapsigargin-treated oocytes mature at similar rates when activated with $\Delta 87$cyclin B1 protein. However, the different responses after cyclin RNA or protein injections could be due to an effect of Ca^{2+}_{cyt} on protein turnover because we injected full-length cyclin B1 RNA and $\Delta 87$cyclin B1 protein, which is missing the first 87 aa and is thus nondegradable because it lacks the destruction box (Kumagai and Dunphy, 1995). Nonetheless, we favor an effect of Ca^{2+}_{cyt} on RNA translation because maturation is enhanced to a similar level when oocytes are activated with Mos or Cyclin B1, two activators that induce the cell cycle kinase cascade at different points.

These data show that Ca^{2+}_{cyt} negatively regulates meiosis entry by acting on at least two sites between PKA inhibition and Mos activation. One site is downstream of PKA inhibition and the other site appears to be mRNA translation, which is required for the induction of the cell cycle machinery (Fig. 7 D). Furthermore, the fact that the rate of maturation is enhanced to a similar extent in oocytes activated with progesterone and PKI (Fig. 7, A and B, PKI) argues that Ca^{2+}_{cyt} acts downstream of PKI (Fig. 7 D).

Ca^{2+}_{cyt} negatively regulates the initiation of the MAPK-MPF cascade

To confirm that Ca^{2+}_{cyt} acts upstream of Mos we analyzed in more details the steps of the cell cycle machinery downstream of Mos in both control and thapsigargin-treated oocytes (Fig. 7 C). As described above MAPK activates significantly earlier in thapsigargin-treated oocytes consistent with the GVBD time course (Fig. 7 C). p90RSK, the downstream substrate of MAPK is activated with a similar time course to MAPK. For these experiments we analyzed lysates form oocytes at GVBD and at $GVBD_{50}$. For the latter time point lysates from oocytes that have undergone GVBD (w)

or not (nw) were collected. Interestingly, p90RSK was phosphorylated to higher levels in the $GVBD_{50}$-nw group in thapsigargin-treated oocytes as compared with controls, thus confirming the earlier activation of the MAPK cascade in thapsigargin-treated oocytes.

Xenopus oocytes contain two pools of cdc2, the catalytic subunit of MPF: the preMPF and the free cdc2 pool. The preMPF pool which is activated at GVBD, contains cdc2 associated with cyclin B. Pre-MPF is kept inactive by phosphorylation on Tyr15 of cdc2 (Nebreda and Ferby, 2000). The free cdc2 pool is activated after association with B-type cyclins synthesized during meiosis I (Hochegger et al., 2001). To determine which pool of cdc2 is activated in thapsigargin-treated oocytes we probed Western blots with a phosphospecific antibody against Tyr15 of cdc2 (Fig. 7 C, P-Y15-cdc2), and determined MPF activity as the H1-kinase activity from $p13^{suc1}$ pulldowns (Fig. 7 C, MPF). In both control and thapsigargin-treated oocytes the disappearance of P-Y15 immunoreactivity coincides with an increase in MPF activity indicating that as in control oocytes the preMPF pool is activated in thapsigargin-treated oocytes. Interestingly, a small level of MPF activity is detected at the $GVBD_{50}$ time point in thapsigargin-treated oocytes that have not undergone GVBD (Fig. 7, Thaps, G50 nw), confirming the early activation of MPF before GVBD observed in Fig. 5.

These data show that in the absence of Ca^{2+}_{cyt} signals the cell cycle kinase cascade downstream of Mos activates normally. Therefore, the more rapid entry into meiosis (GVBD) observed in oocytes deprived of Ca^{2+} signals is due to a negative regulation of Ca^{2+}_{cyt} on the initiation of this kinase cascade upstream of Mos. Blocking Ca^{2+}_{cyt} signals relieves this negative regulation thus allowing more rapid induction of the MAPK-MPF cascade and GVBD.

Discussion

In contrast to the established role of Ca^{2+} signaling in mitosis (Whitaker and Larman, 2001), the requirement for Ca^{2+} in both *Xenopus* and mammalian oocyte meiotic maturation has been difficult to define (Homa et al., 1993; Duesbery and Masui, 1996). To delineate the function of Ca^{2+} during *Xenopus* oocyte meiosis we manipulated Ca^{2+}_{cyt}, extracellular Ca^{2+}, and store Ca^{2+} load and tested the effect on nuclear maturation and the cell cycle machinery. Our data show that Ca^{2+} has two opposing roles during *Xenopus* oocyte maturation: It negatively regulates meiosis entry by delaying the activation of the cell cycle machinery, and it is required for completion of meiosis I (Fig. 7 D).

Ca^{2+}_{cyt} negatively regulates the activation of the cell cycle kinase cascade

Progesterone leads to lower cAMP levels and PKA inhibition within 10 min (Sadler and Maller, 1981), but the next known step in the pathway, that is polyadenylation of maternal RNAs to induce their translation, does not occur until much later (Sheets et al., 1995). The molecular steps during this time lag are not known. Our data show that Ca^{2+}_{cyt} is an important regulator of the transition between PKA inhibition and mRNA translation. Ca^{2+}_{cyt} negatively regulates the activation of the cell cycle machinery by acting on at least two

sites between PKA and Mos (Fig. 7 D). One site of action appears to be mRNA translation. Therefore, the level of Ca^{2+}_{cyt} provides a timing mechanism for entry into meiosis by regulating the initiation of the MAPK-MPF cascade downstream of PKA inhibition (Fig. 7 D). It is tempting to propose that by acting in this capacity Ca^{2+}_{cyt} could synchronize morphological and biochemical changes during oocyte maturation. Under such a scenario, which is completely speculative at this point, Ca^{2+}_{cyt} levels could signal the physiological preparedness of the oocyte to begin maturation. Relatively low Ca^{2+}_{cyt} levels would be indicative of proper functioning of the Ca^{2+} signaling machinery, and thus a healthy oocyte that is ready to mature. In contrast, relatively high Ca^{2+}_{cyt} levels would indicate a compromised oocyte where Ca^{2+}_{cyt} would negatively regulate initiation of maturation. It is interesting in that context that Ca^{2+}_{cyt} acts upstream of Mos, that is before the oocyte activates the cell cycle machinery and commits to maturation. The proposed role of Ca^{2+}_{cyt} in synchronizing morphological and biochemical changes in the oocyte during maturation is further supported by the fact that disrupting Ca^{2+}_{cyt} signaling uncouples the nuclear cell cycle from the MAPK-MPF kinase cascade (Fig. 6).

Ca^{2+}_{cyt} is required for completion of meiosis I

Oocytes deprived of Ca^{2+} signals do not complete meiosis I as they do not extrude a polar body. Rather, they form abnormal spindles early in meiosis I despite normal MAPK and MPF kinetics. This shows that progression through meiosis I requires Ca^{2+}, possibly Ca^{2+} influx before GVBD because oocytes are dependent on extracellular Ca^{2+} only before GVBD (Fig. 6). A Ca^{2+} influx requirement before GVBD fits nicely with the regulation of SOCE during oocyte maturation because SOCE inactivates at the GVBD stage due to MPF activation (Machaca and Haun, 2000, 2002).

Interestingly, others have shown that inhibition of the MAPK cascade (Gross et al., 2000), down-regulation of MPF (Nakajo et al., 2000), or inhibition of protein synthesis (Kanki and Donoghue, 1991) block completion of meiosis I. These treatments lead to a decrease in MPF activity, and induce an interphase-like state that is usually absent between meiosis I and II. In contrast, interfering with Ca^{2+} signaling blocks meiosis I completion, but is not associated with an interphase-like state. Rather, spindle structure is disrupted and polar body formation inhibited, but the chromosomes remain condensed. Furthermore, MPF activity cycles normally with a dip in activity between 1–2 h after GVBD, the expected time for meiosis I to meiosis II transition. These data show that disruption of Ca^{2+} signaling uncouples the cell cycle machinery (MAPK-MPF) from nuclear maturation (i.e., bipolar spindle formation and completion of meiosis I).

It is interesting that the disrupted meiosis I spindle does not activate a spindle checkpoint to arrest the cell cycle. However, there is good evidence against the existence of a meiosis I spindle checkpoint in *Xenopus* oocytes. Blocking the activity of the APC/C or the checkpoint protein Mad2 does not affect progression through meiosis I (Peter et al., 2001; Taieb et al., 2001). This is consistent with our observation of a lack of cell cycle arrest in the absence of Ca^{2+} signals despite disrupted meiosis I spindles.

Recently, Castro et al. (2003) described a similar block of meiosis I after inhibition of Aurora A kinase or its substrate Eg5 (a kinesin-like protein) in *Xenopus* oocytes. Unfortunately, these authors did not assess spindle morphology, but they show that blocking Aurora A inhibits polar body formation with chromosomes maintaining their condensed state long after GVBD (Castro et al., 2003). Members of the Aurora kinase family associate with the spindle and have been shown to be important for both meiosis and mitosis transitions. Therefore, it is possible that Ca^{2+}-dependent pathways somehow modulate Aurora A kinase activity which in turn regulates spindle structure. This possibility remains to be explored.

Role of Ca^{2+} signaling in GVBD

During mitosis NEBD has been shown to be dependent on Ca^{2+} (Poenie et al., 1985; Steinhardt and Alderton, 1988; Twigg et al., 1988; Kao et al., 1990; Wilding et al., 1996), and studies in sea urchin embryos suggest that Ca^{2+} exerts its effect through CaMKII activation (Baitinger et al., 1990). In contrast, during meiosis GVBD is Ca^{2+}-independent as shown here for *Xenopus* oocytes, and in both mouse (Carroll and Swann, 1992; Tombes et al., 1992) and starfish oocytes (Witchel and Steinhardt, 1990). One exception to this rule are some bivalve molluscs where GVBD has been shown to require Ca^{2+} (Deguchi and Osanai, 1994), but unlike amphibian and mammalian oocytes, in this case oocyte maturation and GVBD occur after fertilization which invariably induces a Ca^{2+}_{cyt} rise. Nonetheless, the differential requirement of NEBD on Ca^{2+} signals during meiosis and mitosis is surprising because both NEBD and GVBD require the activation of MPF (Lenart and Ellenberg, 2003), and it is reasonable to assume that the basic structural properties of the nuclear envelope are similar in mitotic and meiotic cells. It has been argued that a Ca^{2+} signal is still required for GVBD but occurs very early or even before the initiation of oocyte maturation in some species (Tombes et al., 1992; Homa et al., 1993). This does not seem to be the case for *Xenopus*, because as shown in Fig. 1 F, eliminating Ca^{2+} signals for as long as 48 h before inducing oocyte maturation has no effect on GVBD, strongly arguing that GVBD is Ca^{2+} independent. Therefore, the differential requirement for Ca^{2+} during the breakdown of the nuclear envelope suggests that NEBD and GVBD are mechanistically distinct.

In conclusion, our results show that Ca^{2+} signals are dispensable for GVBD and chromosome condensation, that Ca^{2+}_{cyt} controls the timing of meiosis entry by negatively regulating the initiation of cell cycle machinery, and that N-Ca^{2+} homeostasis is important for bipolar spindle formation and completion of meiosis I. These results provide a framework to further explore and better define the role of Ca^{2+}-dependent signaling pathways in meiosis and oocyte maturation.

Materials and methods

Oocyte maturation
Xenopus oocytes were obtained as described previously (Machaca and Haun, 2002). The control L-15 solution contains 0.63 mM Ca^{2+}. Ca^{2+} was buffered at 50 μM in the low solution as calculated using the MaxChelator program (http://www.stanford.edu/~cpatton/maxc.html) by the addition of

0.58 mM EGTA. For the H-Ca L-15 solutions Ca^{2+} was added to the indicated concentration as $CaCl_2$. In all experiments, GVBD was visually confirmed by fixing oocytes in methanol and bisecting them in half.

Electrophysiological methods

Recording of the $I_{Ca,Cl}$ was performed as described previously (Machaca and Haun, 2000). $I_{Ca,Cl}$ were recorded in the following solutions: F-Ca contains in micromolars: 96 NaCl, 2.5 KCl, 5 $MgCl_2.6H_2O$, 0.1 EGTA, 10 Hepes, pH 7.4. Low Ca^{2+} Ringer solution (50 μM free Ca^{2+}) contains in micromolars: 96 NaCl, 2.5 KCl, 4.37 $MgCl_2.6H_2O$, 0.63 $CaCl_2.2H_2O$, 0.58 EGTA, 10 Hepes, pH 7.4. Normal Ringer (N-Ca, 0.63 mM Ca^{2+}) and H-Ca solutions (1.5, 3, and 5 mM Ca^{2+}) had the following composition: 96 NaCl, 2.5 KCl, 10 Hepes, pH 7.4; with Ca^{2+} and Mg^{2+} concentrations adding up to 5 mM.

Western blots and MPF kinase assays

MPF kinase activity assay and phospho-MAPK Western blots were prepared as described previously (Machaca and Haun, 2002), except that α-tubulin was used as the loading control for MAPK Western blots. The activation of p90RSK and preMPF was assessed using phosphospecific antibodies against phospho-Thr573 of p90RSK and phospho-Tyr15 of cdc2 (Cell Signaling). MPF activity was also assayed from lysates affinity purified on p13^{suc1} beads using histone-H1 kinase as a substrate essentially as described previously (Howard et al., 1999).

Plasmids and reagents

Heat stable PKI was purchased from Calbiochem. Cyclin B1 and Mos RNAs were synthesized from a pXen-GST-Mos and pSP64-cyclinB1^{xen} plasmids provided by A. Macnicol (University of Arkansas for Medical Sciences; Freeman et al., 1991; Howard et al., 1999) using the mMessage Mmachine transcription kit (Ambion). The His$_6$-tagged Δ87cyclin B1 protein was used as described previously (Machaca and Haun, 2002).

Spindle and polar body staining and image acquisition

Oocytes were fixed in 100% methanol, bisected in half, and incubated in DM1A an antitubulin mAb (Sigma-Aldrich) in TBS containing 2% BSA, followed by a Cy2-conjugated donkey anti–mouse secondary (Jackson ImmunoResearch Laboratory) for 24 h each. The oocytes were washed, dehydrated, stained in 1 μM Sytox® orange (Molecular Probes), and cleared in benzyl alcohol/benzyl benzoate (1:2). Images were collected using a Fluoview confocal (Olympus) coupled to a microscope (model IX70; Olympus) at RT, using a UPlanApo 40× oil objective with an NA of 1.00. The acquisition software was Fluoview 2.1 and figures were compiled using Adobe Photoshop 7.0. For each spindle a z section was obtained and projected onto a single plane to visualize the entire spindle. For polar body emission studies oocytes were fixed in methanol, stained with Sytox® orange, and visualized by confocal microscopy as described for the spindle staining.

References

Arslan, P., F. Di Virgilio, M. Beltrame, R.Y. Tsien, and T. Pozzan. 1985. Cytosolic Ca2+ homeostasis in Ehrlich and Yoshida carcinomas. *J. Biol. Chem.* 260: 2719–2727.

Baitinger, C., J. Alderton, M. Poenie, H. Schulman, and R.A. Steinhardt. 1990. Multifunctional Ca^{2+}/calmodulin-dependent protein kinase is necessary for nuclear envelope breakdown. *J. Cell Biol.* 111:1763–1773.

Camello, C., R. Lomax, O.H. Petersen, and A.V. Tepikin. 2002. Calcium leak from intracellular stores–the enigma of calcium signalling. *Cell Calcium.* 32: 355–361.

Carroll, J., and K. Swann. 1992. Spontaneous cytosolic calcium oscillations driven by inositol trisphosphate occur during in vitro maturation of mouse oocytes. *J. Biol. Chem.* 267:11196–11201.

Castro, A., E. Mandart, T. Lorca, and S. Galas. 2003. Involvement of Aurora A kinase during meiosis I-II transition in *Xenopus* oocytes. *J. Biol. Chem.* 278: 2236–2241.

Ciapa, B., D. Pesando, M. Wilding, and M. Whitaker. 1994. Cell-cycle calcium transients driven by cyclic changes in inositol trisphosphate levels. *Nature.* 368:875–878.

Cicirelli, M.F., and L.D. Smith. 1987. Do calcium and calmodulin trigger maturation in amphibian oocytes? *Dev. Biol.* 121:48–57.

Coleman, T.R., and W.G. Dunphy. 1994. Cdc2 regulatory factors. *Curr. Opin. Cell Biol.* 6:877–882.

Cork, R.J., M.F. Cicirelli, and K.R. Robinson. 1987. A rise in cytosolic calcium is not necessary for maturation of *Xenopus laevis* oocytes. *Dev. Biol.* 121:41–47.

Deguchi, R., and K. Osanai. 1994. Meiosis reinitiation from the first prophase is dependent on the levels of intracellular Ca2+ and pH in oocytes of the bivalves Mactra chinensis and Limaria hakodatensis. *Dev. Biol.* 166:587–599.

Duesbery, N.S., and Y. Masui. 1996. The role of Ca^{2+} in progesterone-induced germinal vesicle breakdown of *Xenopus laevis* oocytes: the synergic effects of microtubule depolymerization and Ca^{2+}. *Dev. Genes Evol.* 206:110–124.

Freeman, R.S., S.M. Ballantyne, and D.J. Donoghue. 1991. Meiotic induction by *Xenopus* cyclin B is accelerated by coexpression with mosXe. *Mol. Cell. Biol.* 11:1713–1717.

Gross, S.D., M.S. Schwab, F.E. Taieb, A.L. Lewellyn, Y.W. Qian, and J.L. Maller. 2000. The critical role of the MAP kinase pathway in meiosis II in *Xenopus* oocytes is mediated by p90(Rsk). *Curr. Biol.* 10:430–438.

Hochegger, H., A. Klotzbucher, J. Kirk, M. Howell, K. le Guellec, K. Fletcher, T. Duncan, M. Sohail, and T. Hunt. 2001. New B-type cyclin synthesis is required between meiosis I and II during *Xenopus* oocyte maturation. *Development.* 128:3795–3807.

Homa, S.T., J. Carroll, and K. Swann. 1993. The role of calcium in mammalian oocyte maturation and egg activation. *Hum. Reprod.* 8:1274–1281.

Howard, E.L., A. Charlesworth, J. Welk, and A.M. MacNicol. 1999. The mitogen-activated protein kinase signaling pathway stimulates mos mRNA cytoplasmic polyadenylation during *Xenopus* oocyte maturation. *Mol. Biol. Cell.* 19:1990–1999.

Kanki, J.P., and D.J. Donoghue. 1991. Progression from meiosis I to meiosis II in *Xenopus* oocytes requires *de novo* translation of the *mos*^{xe} protooncogene. *Proc. Natl. Acad. Sci. USA.* 88:5794–5798.

Kao, J.P., J.M. Alderton, R.Y. Tsien, and R.A. Steinhardt. 1990. Active involvement of Ca^{2+} in mitotic progression of Swiss 3T3 fibroblasts. *J. Cell Biol.* 111:183–196.

Kumagai, A., and W.G. Dunphy. 1995. Control of the Cdc2/cyclin B complex in *Xenopus* egg extracts arrested at a G2/M checkpoint with DNA synthesis inhibitors. *Mol. Biol. Cell.* 6:199–213.

Lenart, P., and J. Ellenberg. 2003. Nuclear envelope dynamics in oocytes: from germinal vesicle breakdown to mitosis. *Curr. Opin. Cell Biol.* 15:88–95.

Machaca, K., and H.C. Hartzell. 1999. Reversible Ca gradients between the subplasmalemma and cytosol differentially activate Ca-dependent Cl currents. *J. Gen. Physiol.* 113:249–266.

Machaca, K., and S. Haun. 2000. Store-operated calcium entry inactivates at the germinal vesicle breakdown stage of *Xenopus* meiosis. *J. Biol. Chem.* 275: 38710–38715.

Machaca, K., and S. Haun. 2002. Induction of maturation-promoting factor during *Xenopus* oocyte maturation uncouples Ca^{2+} store depletion from store-operated Ca^{2+} entry. *J. Cell Biol.* 156:75–86.

Machaca, K., Z. Qu, A. Kuruma, H.C. Hartzell, and N. McCarty. 2001. The endogenous calcium-activated Cl channel in *Xenopus* oocytes: a physiologically and biophysically rich model system. *In* Calcium Activates Chloride Channels. C.M. Fuller, editor. Academic Press, San Diego. 3–39.

Means, A.R. 1994. Calcium, calmodulin and cell cycle regulation. *FEBS Lett.* 347: 1–4.

Moreau, M., M. Doree, and P. Guerrier. 1976. Electrophoretic introduction of calcium into the cortex of *Xenopus laevis* oocytes triggers meiosis reinitiation. *J. Exp. Zool.* 197:443–449.

Moreau, M., J.P. Vilain, and P. Guerrier. 1980. Free calcium changes associated with hormone action in amphibian oocytes. *Dev. Biol.* 78:201–214.

Nakajo, N., S. Yoshitome, J. Iwashita, M. Iida, K. Uto, S. Ueno, K. Okamoto, and N. Sagata. 2000. Absence of Wee1 ensures the meiotic cell cycle in *Xenopus* oocytes. *Genes Dev.* 14:328–338.

Nebreda, A.R., and I. Ferby. 2000. Regulation of the meiotic cell cycle in oocytes. *Curr. Opin. Cell Biol.* 12:666–675.

O'Connor, C.M., K.R. Robinson, and L.D. Smith. 1977. Calcium, potassium, and sodium exchange by full-grown and maturing *Xenopus laevis* oocytes. *Dev. Biol.* 61:28–40.

Parekh, A.B., and R. Penner. 1997. Store depletion and calcium influx. *Physiol. Rev.* 77:901–930.

Peter, M., A. Castro, T. Lorca, C. Le Peuch, L. Magnaghi-Jaulin, M. Doree, and J.C. Labbe. 2001. The APC is dispensable for first meiotic anaphase in *Xenopus* oocytes. *Nat. Cell Biol.* 3:83–87.

Picard, A., F. Giraud, F. Le Bouffant, F. Sladeczek, C. Le Peuch, and M. Doree. 1985. Inositol 1,4,5-trisphosphate microinjection triggers activation, but not meiotic maturation in amphibian and starfish oocytes. *FEBS Lett.* 182:446–450.

Poenie, M., J.M. Alderton, R.Y. Tsien, and R.A. Steinhardt. 1985. Changes of free calcium levels with stages of the cell division cycle. *Nature.* 315:147–149.

Robinson, K.R. 1985. Maturation of *Xenopus* oocytes is not accompanied by electrode-detectable calcium changes. *Dev. Biol.* 109:504–508.

Sadler, S.E., and J.L. Maller. 1981. Progesterone inhibits adenylate cyclase in *Xenopus* oocytes. Action on the guanine nucleotide regulatory protein. *J. Biol. Chem.* 256:6368–6373.

Schorderet-Slatkine, S., M. Schorderet, and E.E. Baulieu. 1976. Initiation of meiotic maturation in *Xenopus laevis* oocytes by lanthanum. *Nature.* 262:289–290.

Sheets, M.D., M. Wu, and M. Wickens. 1995. Polyadenylation of c-mos mRNA as a control point in *Xenopus* meiotic maturation. *Nature.* 374:511–516.

Soboloff, J., and S.A. Berger. 2002. Sustained ER Ca²⁺ depletion suppresses protein synthesis and induces activation-enhanced cell death in mast cells. *J. Biol. Chem.* 277:13812–13820.

Steinhardt, R.A., and J.M. Alderton. 1988. Intracellular free calcium rise triggers nuclear envelope breakdown in the sea urchin embryo. *Nature.* 332:364–366.

Stricker, S.A. 2000. Comparative biology of calcium signaling during fertilization and egg activation in animals. *Dev. Biol.* 211:157–176.

Taieb, F.E., S.D. Gross, A.L. Lewellyn, and J.L. Maller. 2001. Activation of the anaphase-promoting complex and degradation of cyclin B is not required for progression from Meiosis I to II in *Xenopus* oocytes. *Curr. Biol.* 11:508–513.

Tombes, R.M., C. Simerly, G.G. Borisy, and G. Schatten. 1992. Meiosis, egg activation, and nuclear envelope breakdown are differentially reliant on Ca²⁺, whereas germinal vesicle breakdown is Ca²⁺ independent in the mouse oocyte. *J. Cell Biol.* 117:799–811.

Tunquist, B.J., and J.L. Maller. 2003. Under arrest: cytostatic factor (CSF)-mediated metaphase arrest in vertebrate eggs. *Genes Dev.* 17:683–710.

Twigg, J., R. Patel, and M. Whitaker. 1988. Translational control of InsP3-induced chromatin condensation during the early cell cycles of sea urchin embryos. *Nature.* 332:366–369.

Wasserman, W.J., and Y. Masui. 1975. Initiation of meiotic maturation in *Xenopus laevis* oocytes by the combination of divalent cations and ionophore A23187. *J. Exp. Zool.* 193:369–375.

Wasserman, W.J., and L.D. Smith. 1981. Calmodulin triggers the resumption of meiosis in amphibian oocytes. *J. Cell Biol.* 89:389–394.

Wasserman, W.J., L.H. Pinto, C.M. O'Connor, and L.D. Smith. 1980. Progesterone induces a rapid increase in [Ca²⁺]in of *Xenopus laevis* oocytes. *Proc. Natl. Acad. Sci. USA.* 77:1534–1536.

Whitaker, M. 1995. Regulation of the cell division cycle by inositol trisphosphate and the calcium signaling pathway. *Adv. Second Messenger Phosphoprotein. Res.* 30:299–310.

Whitaker, M., and M.G. Larman. 2001. Calcium and mitosis. *Semin. Cell Dev. Biol.* 12:53–58.

Wilding, M., E.M. Wright, R. Patel, G. Ellis-Davies, and M. Whitaker. 1996. Local perinuclear calcium signals associated with mitosis-entry in early sea urchin embryos. *J. Cell Biol.* 135:191–199.

Witchel, H.J., and R.A. Steinhardt. 1990. 1-Methyladenine can consistently induce a fura-detectable transient calcium increase which is neither necessary nor sufficient for maturation in oocytes of the starfish Asterina miniata. *Dev. Biol.* 141:393–398.

Yamashita, M., K. Mita, N. Yoshida, and T. Kondo. 2000. Molecular mechanisms of initiation of oocyte maturation: general and species-specific aspects. *Prog. Cell Cycle Res.* 4:115–129.